Preprints of the 10th IFAC International Symposium on Dynamics and Control of Process Systems
The International Federation of Automatic Control
December 18-20, 2013. Mumbai, India

A Grey-Box Model for Spray Drying Plants

Lars Norbert Petersen *,** **Niels Kjølstad Poulsen** *
Hans Henrik Niemann *** **Christer Utzen** **
John Bagterp Jørgensen *

* *Department of Applied Mathematics and Computer Science, Technical University of Denmark, Kgs. Lyngby, Denmark (e-mail: {lnpe,nkpo,jbjo}@dtu.dk)*
** *GEA Process Engineering A/S, Søborg, Denmark (e-mail: christer.utzen@gea.com)*
*** *Department of Electrical Engineering, Technical University of Denmark, Kgs. Lyngby, Denmark (e-mail: hhn@elektro.dtu.dk)*

Abstract: Multi-stage spray drying is an important and widely used unit operation in the production of food powders. In this paper we develop and present a dynamic model of the complete drying process in a multi-stage spray dryer. The dryer is divided into three stages: The spray stage and two fluid bed stages. Each stage is assumed ideally mixed and described by mass- and energy balances. The model is able to predict the temperature, the residual moisture and the particle size in each stage. Process constraints are also proposed to predict deposits due to stickiness of the powder. The model predictions are compared to datasets gathered at GEA Process Engineering's test facility. The identified grey-box model parameters are identified from data and the resulting model fits the data well. The complexity of the model has been selected such that it is suitable for development of real-time optimization algorithms in an economic optimizing MPC framework.

Keywords: Drying process, Spray drying, Multi-stage dryer, Grey-box model, Modelling and identification, Maltodextrin, Simulation

1. INTRODUCTION

In 2015 the milk quota system in the European Union will be completely liberalized. The expected effect is that the milk volume production will increase significantly. The extra milk will need to be processed to find its way to the market. Analysts expect production of skimmed and whole milk powder to increase by 5-6% while its prices will decline by about 6-7% (IPTS and EuroCARE GmbH, 2009). To accommodate this production expansion, efficient control and optimization of the spray drying process become increasingly important. In this paper we develop a simple first-principle engineering model that can be used to simulate the spray drying processes and facilitate development of efficient control algorithms.

In this paper a grey-box model will be introduced which is based on engineering first principles. It describes the spray drying (SD), the static fluid bed (SFB) and the vibrating fluid bed (VFB) stages of a multi-stage dryer (MSD) plant as illustrated in Fig. 1. The model is validated against data acquired from a MSD at a test-station in Copenhagen (GEA Process Engineering A/S). The model describes the temperatures, the residual moisture and the particle size in each stage of the spray dryer, as well as the stickiness limit.

Conventional control of spray drying plants keeps inlet- and outlet temperatures constant during operation, as a surrogate to controlling the product quality (O'Callaghan and Cunningham, 2005). This approach is simple, but known to be insufficient for control of residual moisture and particle size. The simple approach is often preferred, as product quality is expensive to measure and can lead to sanitary problems. One approach to avoid the use of expensive sensors is to use soft sensors based on readily available measurements and a mathematical model. The importance of good models is therefore evident for both use in controllers and soft sensors as well as in design and validation studies.

Chen and Lin (2005) derived a simple set of differential equations for use in computational fluid dynamics (CFD) to describe the drying of a single particle. In this study, it was shown that the characteristic drying rate curve (CDRC) method did not resemble the experimental trends, and therefore they preferred the reaction engineering approach (REA) method. Langrish (2009) used the REA method for CFD with success on studying wall depositions. Shabde and Hoo (2008) investigated control design and optimization using CFD methods for a single-stage spray dryer, and described a (lumped) model and control for the residual moisture and the particle size. We deemed the models relying on CFD too complex for real-time advanced control and real-time dynamic optimization. Bizmark et al. (2010) introduced a sequential static model for a continuous fluidized bed and Iguaz et al. (2003) formulated a sequential reactor approach, which was used to simulate the dynamic response of a rotary dryer to a change in the input conditions. We come up with a three-stage approach inspired by Bizmark et al. (2010) and Iguaz

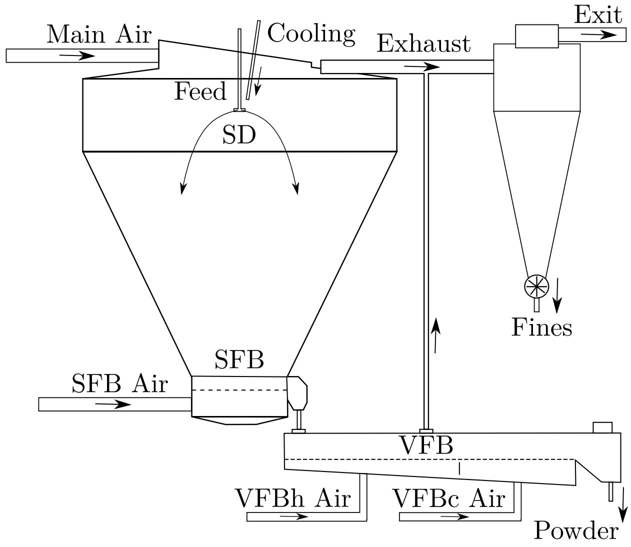

Fig. 1. Diagram of the multi-stage dryer. SD = spray drying, SFB = static fluid bed and VFB = vibrating fluid bed

et al. (2003) and use constitutive equations inspired by Langrish and Kockel (2001).

To our knowledge, no control oriented general dynamic model exist for multi-stage spray dryers. In this work such a general model is proposed.

The paper is organized as follows. In Section 2 we describe the spray drying process and in Section 3 we present the three-stage model. We also give constraints to the residual moisture in order to predict wall deposits. Section 4 contains a brief description of the method for parameter estimation, the estimated parameters, and a validation of the model to data from two experiments. Conclusions are given in Section 5.

2. THE SPRAY DRYING PROCESS

As illustrated in Fig. 1, spray drying is a continuous process which produces a dry powder from a liquid or a slurry. The spray dryer consists most often of a combination of three stages; the actual spray drying (SD), the static fluid bed (SFB) and the vibrating fluid bed (VFB). The main purpose of the SD stage is to reduce stickiness and fouling of the wet feed. The powder then falls to the SFB for further agglomeration and drying. Finally the powder is transported to the external VFB, for gentle drying and is cooled to the temperature desired for handling and storage. Cooling air and fines from the cyclone are returned to the SD stage near the nozzles for forced agglomeration.

The main factors affecting the residual moisture in the powder are the temperature, the relative humidity and the particle size in the stages. Normally, the SD air temperature (exhaust temperature) is automatically controlled by adjusting the feed flow rate while the temperatures in the other stages are manually controlled from the inlet air temperatures set by the operator. The particle size is mainly affected by the nozzle pressure (i.e. feed flow, concentration and viscosity), residual moisture and the SFB inlet air flows. The particle size is often controlled by adjusting inlet air flows and the residual moisture is controlled from the exhaust temperature. Generally, two external disturbances are present in spray drying i.e. the ambient air humidity and the feed composition. The disturbances both affect the residual moisture and the particle size. Also the hold-up of powder in the SFB and VFB can vary and influences the drying.

3. MULTI-STAGE DRYER MODEL

The model structure is derived from engineering first principles and the unknown parameters are identified using a least-squares method. This approach, called grey-box modeling (Ljung, 1999), combines physical knowledge with data-based (statistical) modeling; physical knowledge provides the main structure and statistical modeling provides details on the actual coefficients (Kristensen et al., 2004). Compared to statistical black-box models; this is advantageous since it allows a physical interpretation of the model and often wide valid operation range. Utilizing mass and energy conservation laws, also make it possible to extract otherwise unknown drying conditions inside the drying zones.

We divide the model of the dryer into three stages. The SD, the SFB and the VFB stage. Fig. 2 shows a schematic representation of the three-stage model approach, and Fig. 3 describes the details of a single stage.

For each of the stages, we set up two mass balances (Eq. 1 and 4), one energy balance (Eq. 15) and one particle size balance (Eq. 31) in order to fully describe the drying conditions in each stage. In the following, the derivation of the equations for the stages will be treated generally and when necessary a specific stage is noted in the superscript of the equation.

The experiments were based on drying of maltodextrin DE-18, because milk is expensive, cannot be stored in liquid form and its composition is not well defined. Maltodextrin, though, resemble the same fundamental properties as skim milk.

3.1 Powder moisture

A mass balance for water in the powder yields

$$\frac{dm_w}{dt} = F_{ps_{in}}X_{in} - F_{ps_{out}}X_{out} - R_w m_{ps} \tag{1}$$

X is the dry basis water concentration (kg water/kg dry solid) in the powder and the flux of evaporating water is $R_w m_{ps}$. The hold-up of dry powder is assumed constant, and thus the flow of dry powder entering and leaving is

$$F_{ps_{out}} = F_{ps_{in}} = S_{in}F_{p_{in}} \tag{2}$$

The dry basis concentration of product in- and outlet flows are

$$X_{in} = \frac{1 - S_{in}}{S_{in}} \qquad X_{out} = \frac{m_w}{m_p - m_w} \tag{3}$$

where S_{in} is the concentration (kg solid/kg total) and m_w is the mass of water. m_p is the total mass of the powder.

3.2 Air moisture

The amount of vapour in the air is given by

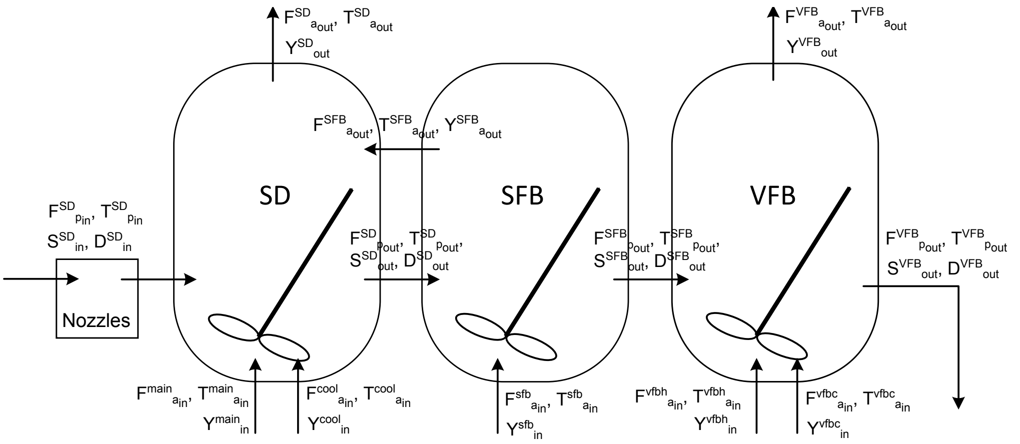

Fig. 2. Princple of the sequential stage model.

$$\frac{dm_v}{dt} = F_{v_{in}} - F_{v_{out}} + R_w m_{ps} \tag{4}$$

The inlet vapour flow, $F_{v_{in}}$, for each stage is

$$F_{v_{in}}^{SD} = Y_{in}^{main} F_{da_{in}}^{main} + Y_{in}^{cool} F_{da_{in}}^{cool} + Y_{out}^{SFB} F_{da_{out}}^{SFB} \tag{5}$$

$$F_{v_{in}}^{SFB} = Y_{in}^{sfb} F_{da_{in}}^{sfb} \tag{6}$$

$$F_{v_{in}}^{VFB} = Y_{in}^{vfbh} F_{da_{in}}^{vfbh} + Y_{in}^{vfbc} F_{da_{in}}^{vfbc} \tag{7}$$

The flow of dry air, $F_{da_{in}}$, is given by

$$F_{da_{in}} = \frac{1}{Y_{in}+1} F_{a_{in}} \tag{8}$$

and the absolute humidity, Y_{in}, of the incoming air is

$$Y_{in} = \frac{M_v}{M_{da}} \frac{\mathrm{RH}_{in} P_{vsat}}{P_{in} - \mathrm{RH}_{in} P_{vsat}} \tag{9}$$

RH_{in} is the relative humidity and P_{vsat} is the saturated vapour pressure from the Antoine equation.

The hold-up of dry air is assumed constant, and thus the dry air flow out of the chamber is equal to the dry air flow into the chamber. The flow of vapour out of the stages is

$$F_{v_{out}}^{SD} = Y_{out}^{SD} (F_{da_{in}}^{main} + F_{da_{in}}^{cool} + F_{da_{out}}^{SFB}) \tag{10}$$

$$F_{v_{out}}^{SFB} = Y_{out}^{SFB} F_{da_{in}}^{sfb} \tag{11}$$

$$F_{v_{out}}^{VFB} = Y_{out}^{VFB} (F_{da_{in}}^{vfbh} + F_{da_{in}}^{vfbc}) \tag{12}$$

The absolute humidity of the stage air, Y_{out}, is given by

$$Y_{out} = \frac{M_{da}}{M_v} \frac{P - P_v}{P_v} \tag{13}$$

Assuming constant total chamber pressure, P, which is controlled by a suction fan. The vapour pressure is given by the ideal gas law

$$P_v = \frac{M_v R T_{a_{out}}}{m_v V} \tag{14}$$

M_v is the molar mass of vapour. V is the stage air volume.

3.3 Energy balance

It is assumed that in each stage the temperature of the air and the product are in equilibrium and identical. This temperature is defined by an energy balance

$$\frac{dU}{dt} = \Delta H + Q + W \tag{15}$$

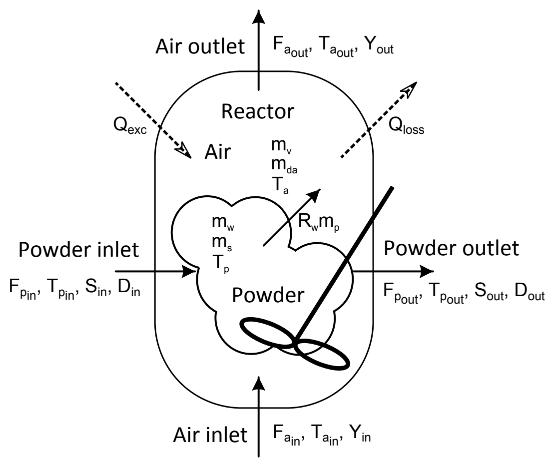

Fig. 3. Sketch of a single stage.

where $W = 0$ and

$$\Delta H = H_{a_{in}} - H_{a_{out}} + H_{p_{in}} - H_{p_{out}} \tag{16}$$

$$Q = -Q_{loss} + Q_{exc} \tag{17}$$

The enthalpy of humid air is

$$H_a = H_{a_0} + F_{da}(C_{da}(T_a - T_{ref}) + Y(\lambda + C_v(T_a - T_{ref}))) \tag{18}$$

where C_{da} and C_v is the specific heat capacity of dry air and vapour respectively. λ is the latent heat of evaporation and $T_{ref} = 25°C$ is the reference temperature.

The enthalpy increase from inlet air in each stage is

$$H_{a_{in}}^{SD} = H_{a_{in}}^{main} + H_{a_{in}}^{cool} + H_{a_{out}}^{SFB} \tag{19}$$

$$H_{a_{in}}^{SFB} = H_{a_{in}}^{sfb} \tag{20}$$

$$H_{a_{in}}^{VFB} = H_{a_{in}}^{vfbh} + H_{a_{in}}^{vfbc} \tag{21}$$

The enthalpy of humid air leaving the stages is simply determined from (18). We denote the enthalpies $H_{a_{out}}^{SD}$, $H_{a_{out}}^{SFB}$ and $H_{a_{out}}^{VFB}$.

The enthalpy of liquid feed as well as powder is

$$H_p = H_{p_0} + F_{ps}(C_s + XC_w)(T_p - T_{ref}) \tag{22}$$

where C_s and C_w is the specific heat capacity of solids and water respectively.

The heat loss is given by

$$Q_{loss} = UA(T_{a_{out}} - T_{indoor}) \tag{23}$$

Since the indoor temperature was not measured, we approximate the indoor temperature by T_{vfbc}.

The SD and SFB stage is subject to exchange of heat, as these are placed inside the same chamber. The heat exchange is

$$Q_{exc}^{SD} = -UA_{exc}(T_{a_{out}}^{SD} - T_{a_{out}}^{SFB}) \tag{24}$$

$$Q_{exc}^{SFB} = UA_{exc}(T_{a_{out}}^{SD} - T_{a_{out}}^{SFB}) \tag{25}$$

The VFB is isolated from the other stages, and thus have zero heat exchange i.e. $Q_{exc}^{VFB} = 0$.

The total energy is given by

$$U = m_p C_p T_{p_{out}} + m_{da} C_{da} T_{a_{out}} + m_v C_{av} T_{a_{out}} + m_{steel} C_{steel} T_{a_{out}} \tag{26}$$

As mentioned the temperature of the air in the chamber, $T_{a_{out}}$ equals $T_{p_{out}}$. The heat capacities are placed in appendix A. In this we assume that the temperature of the steel chamber changes reasonably fast compared to the air temperature. The mass of steel is determined by assuming 3 mm of steel. i.e. $m_{steel}^{SD} = 212.22$ kg, $m_{steel}^{SFB} = 7.80$ kg and $m_{steel}^{VFB} = 8.10$ kg.

3.4 Drying rate equation

The evaporation rate, R_w, is an essential part of the model. According to Iguaz et al. (2003) it should include equilibrium moisture content data and must be determined experimentally under conditions as close as possible to those of the process. We find that the drying kinetics is best described by the lumped-parameter expression (Langrish and Kockel, 2001; Chen and Lin, 2005). Thus, the drying rate is a function of vapour density and the moisture content. The drying rate may be expressed as

$$R_w = K_1(X_{out} - X_{eq})(\rho_{vsat} - \rho_v) \tag{27}$$

where

$$\rho_{vsat} = \frac{M_v P_{vsat}}{RT_{p_{out}}} \qquad \rho_v = \frac{M_v P_v}{RT_{a_{out}}} \tag{28}$$

The last term of (27), $\rho_{vsat} - \rho_v$, describes the driving force of evaporation from the particles to the air, assuming that the surface of the particle is completely covered in water. To describe the friction of evaporation we introduce the term of free moisture, $X_{out} - X_{eq}$. The term decreases towards zero as the residual moisture get closer to the equilibrium moisture content. The constant K_1 corrects for un-modelled effects, such as relative speed between air and particle and other phenomena affecting drying. These phenomena are practically impossible to model without taking a CFD approach. It is, furthermore, necessary to multiply R_w by $F_{p_{in}}^{SD}/0.0241$ in the SD stage in order to correctly render variations in the feed flow.

The equilibrium moisture content, X_{eq}, is described by

$$X_{eq} = A\left(\frac{RH_{a_{out}}}{1 - RH_{a_{out}}}\right)^B \left(\frac{1}{T_{a_{out}} - 273.15}\right)^C \tag{29}$$

X_{eq} is a product dependent function that describe the moisture content where water cannot be extracted from the powder any longer. As the moisture content approaches this value the friction of extracting water from the particles increase to infinite. In theory the moisture content can only be obtained by infinite residence time. Woo et al. (2008), shows that $A = 1.2098$, $B = 0.8535$ and $C = 0.5962$ can be used for maltodextrin DE-18.

3.5 Particle size

The droplets can be produced by either a rotating atomizer or a nozzle. We use a nozzle and the particle size can be described by

$$D_{in}^{SD} = D_0 + a(F_{p_{in}}^{SD} - F_{p0}) + b(T_{p_{in}}^{SD} - T_{p0}) + c(S_{in}^{SD} - S_0) \tag{30}$$

The constants have been manually fitted to

$$a = 4000 \qquad b = -10.1 \qquad c = -600$$
$$F_{p0} = 0.021921 \qquad T_{p0} = 326.35 \qquad S_0 = 0.5$$

The sprayed droplets are subject to shrinkage during drying. If it is assumed that the particles are perfectly spherical before and after the drying and only water is evaporating, we can derive a differential equation for the resulting size of the particles. For each stage we get

$$\dot{D}_{out} = \frac{1}{\tau}\left(\left(\frac{X_{out}+1}{X_{in}+1} \cdot \frac{\rho_{p_{in}}}{\rho_{p_{out}}}\right)^{\frac{1}{3}} D_{in} + K_{ag}(F_a - F_{a0}) - D_{out}\right) \tag{31}$$

Agglomeration is generally difficult to describe and we simply add a term proportional to the air flow rate of the stage. The parameters are

$$\tau^{SD} = 400 \qquad \tau^{SFB} = 200 \qquad \tau^{VFB} = 100$$
$$K_{ag}^{SD} = 100 \qquad K_{ag}^{SFB} = 300 \qquad K_{ag}^{VFB} = 200$$
$$F_{a0}^{SD} = 0.49944 \quad F_{a0}^{SFB} = 0.14167 \quad F_{a0}^{VFB} = 0.18046$$

3.6 Stickiness

Stickiness of the produced particles is an important limitation to the achievable performance of the MSD. Sticky particles form depositions on the walls of the spray dryer. Stickiness has been found to depend on product temperature and moisture content. Furthermore, the transition from sticky to non-sticky takes place very quickly, thus we can assume it to have binary state. We will use a mass-proportion-mixing rule, as proposed by (Hennigs et al., 2001; Hogan et al., 2010), to describe the non-sticky region i.e. when the powder is below its glass transition temperature.

$$T_g = \frac{S_{out}T_{gp} + k(1 - S_{out})T_{gw}}{S_{out} + k(1 - S_{out})} \tag{32}$$

$T_{gp} = 144.8°C$ and $T_{gw} = -137°C$ for maltodextrin DE-18 and water respectively. The value $k = 6.296$ is estimated from adsorption isotherm data.

The data of the experiment is produced by studying the stickiness of the powder in an equilibrium state. Meaning that the moisture at the surface is equal to that of the core of the particle. This situation is not present in spray drying, where the rapid evaporation from the surface tend to form a particle with a crisper surface than the core. In practice this means that T_g is higher i.e. that the powder is less sticky inside the spray dryer. To compensate for this, we form a correction term

$$T_{max} = T_g + \Delta T_{adj} \tag{33}$$

The offset depends on the design of the dryer and unknown factors. Normally it is in the range of 10 to 60°C (Hogan

Table 1. Identified parameters.

Symbol	Value	99% Conf.	Unit
K_1	0.027106	± 0.00070505	$m^3/(s \cdot kg)$
U^{SD}	6.0576	± 0.05556	J/Km^2
U^{SFB}	56.513	± 0.67788	J/Km^2
U^{VFB}	151.74	± 4.1353	J/Km^2
m_p^{SD}	19.279	± 0.45641	kg
m_p^{SFB}	15.954	± 1.8596	kg
m_p^{VFB}	3.4953	± 3.7004	kg
UA_{exc}	113.76	± 3.0285	J/K
D_0	154.39	± 0.12645	μm

et al., 2010). It must be determined experimentally for each dryer.

4. SYSTEM IDENTIFICATION

The unknown variables in the grey-box model are identified in order to determine the relation between input and output variables of the MSD. The cost function is the sum of squared prediction errors. The dynamic system is described by the set of ordinary differential equations (ODEs) given in Section 3. Consequently, the grey-box model of the MSD can be written

$$\frac{d}{dt}\mathbf{x}(t) = \mathbf{f}(\mathbf{x}(t), \mathbf{u}(t), \theta)$$
$$\widehat{\mathbf{y}}(t_k) = \mathbf{g}(\mathbf{x}(t_k), \mathbf{u}(t_k), \theta)$$

with the optimization problem given by

$$\mathbf{e}(t_k, \theta) = \mathbf{y}(t_k) - \widehat{\mathbf{y}}(t_k, \theta)$$
$$V_{LS}(\theta) = \frac{1}{2}\sum_{t_k=1}^{N} \|\mathbf{e}(t_k, \theta)\|^2_{\mathbf{w}}$$
$$\widehat{\theta}_{LS} = \arg\min_{\theta \in D_m} V_{LS}(\theta)$$

$\mathbf{y}(t_k)$ and $\widehat{\mathbf{y}}(t_k, \theta)$ are the measured and estimated output at time t_k. We ignore the initial startup trend i.e. only use data points from $t_k > 5.8$ hours. $\mathbf{e}$ is the estimation error (residual) and V_{LS} is the value of the cost function. The weights have been selected to

$$\mathbf{w} = diag([1\ 1\ 1\ 100\ 0.05])$$

The weights are selected such that the magnitude of the residuals are in the same range. The weight on S^{SFB}_{out} could be increased, giving a better fit on this residual. But then the temperature estimates will suffer and vice versa. The outputs and inputs are

$$\mathbf{y} = \left[T^{SD}_{a_{out}}\ T^{SFB}_{p_{out}}\ T^{VFB}_{a_{out}}\ S^{SFB}_{out}\ D^{SFB}_{out}\right]^T$$
$$\mathbf{u} = [F^{feed}\ T^{feed}\ S^{feed}\ F^{main}\ T^{main}\ Y^{main}\ F^{cool}\ \dots$$
$$T^{cool}\ Y^{cool} F^{sfb}\ T^{sfb}\ Y^{sfb}\ F^{vfbh}\ T^{vfbh}\ \dots$$
$$Y^{vfbh}\ F^{vfbc}\ T^{vfbc}\ Y^{vfbc}\ T_{indoor}]^T$$
$$\mathbf{x} = [m^{SD}_w\ m^{SD}_v\ T^{SD}_{a_{out}}\ D^{SD}_{out}\ m^{SFB}_w\ m^{SFB}_v\ T^{SFB}_{a_{out}}\ \dots$$
$$D^{SFB}_{out}\ m^{VFB}_w\ m^{VFB}_v\ T^{VFB}_{a_{out}}\ D^{VFB}_{out}]^T$$

The identified parameters are shown in Table 1. The approximate 99% confidence interval in Table 1 is given by $p_i \pm t_{m-n}\hat{\sigma}\sqrt{C^{-1}_{ii}}$ with $m - n = 1525 - 9$ equal to the degrees of freedom, t is the student-T-distribution, $\hat{\sigma}$ is the unbiased estimate of the noise covariance and $C = J^T J$ where J is the Jacobian of the model.

The correlation matrix for the parameters is

$$\begin{bmatrix} 1 \\ -0.35 & 1 \\ 0.19 & -0.95 & 1 \\ 0.33 & -0.36 & 0.28 & 1 \\ -0.36 & -0.59 & 0.64 & 0.18 & 1 \\ 0.46 & -0.44 & 0.24 & 0.41 & 0.15 & 1 \\ 0.02 & -0.09 & 0.08 & 0.74 & 0.09 & 0.06 & 1 \\ 0.04 & -0.49 & 0.61 & 0.03 & 0.00 & 0.05 & 0.01 & 1 \\ 0.63 & -0.67 & 0.51 & 0.47 & 0.31 & 0.83 & 0.08 & 0.05 & 1 \end{bmatrix}$$

The hold-up of powder in the VFB, m^{VFB}_p, is difficult to estimate, as it is mostly determined from a combination of the measurement of residual moisture in the VFB (unmeasured) and the dynamic change of temperature $T^{VFB}_{a_{out}}$, which is slowly varying.

Fig. 4 shows the estimation data and the corresponding model response. The model response to the validation data is shown in Fig. 5. We removed a constant temperature offset in the validation model response by adjusting the indoor temperature by $\Delta T^{SD}_{indoor} = -10.06°C$, $\Delta T^{SFB}_{indoor} = 14.33°C$ and $\Delta T^{SFB}_{indoor} = 2.745°C$. The reason for these offsets is most likely the changed indoor temperature between trials (the dryer is placed in a tall unheated test-facility) and the non-uniform temperature between top and bottom of the dryer. The indoor temperature was unfortunately not measured.

The estimation dataset (Fig. 4) is made by first changing the SD feed flow from 65 l/h to 75 l/h twice. The inlet air temperature is then changed from 160°C to 150°C and increased to 170°C and back. The SD air flow is then changed from 1800 kg/h to 2000 kg/h and back twice. The second time with the heater in manual, which cause the inlet air temperature to drop slightly. Then the SFB inlet air flow was changed followed by a change in the SFB inlet air temperature.
In the validation dataset (Fig. 5) the SD outlet air temperature is controlled constant at 87°C by the feed flow rate. First the inlet air humidity is changed from 7 to 22 g/kg and back. Next the feed solids content is changed from 50% to 40% and back. Notice the difference in time-scale of the two experiments.

Inspecting Fig. 4 and 5, we conclude that the estimation of temperatures shows a precise fit while the product quality is more difficult to estimate. Disregarding the initial start-up trend of approx. 4-5 hours, in which the dryer is not operating normally, especially the residual moisture is difficult to estimate. The reason is the difficulty of measuring the residual moisture, the indoor temperature change and the discontinuous discharge (especially in the validation data at $t = 4.5$) of powder from the SFB. The estimation of particle size is slightly off, but within reasonable limits. For a greater accuracy we might need to model the nozzle pressure directly and the fines return system.

As a consequence the MSD is now being upgraded with in-line residual moisture sensors, indoor temperature sensors and a new mechanism for discharge of powder from the SFB. A new experiment has already been ordered and will soon be conducted.

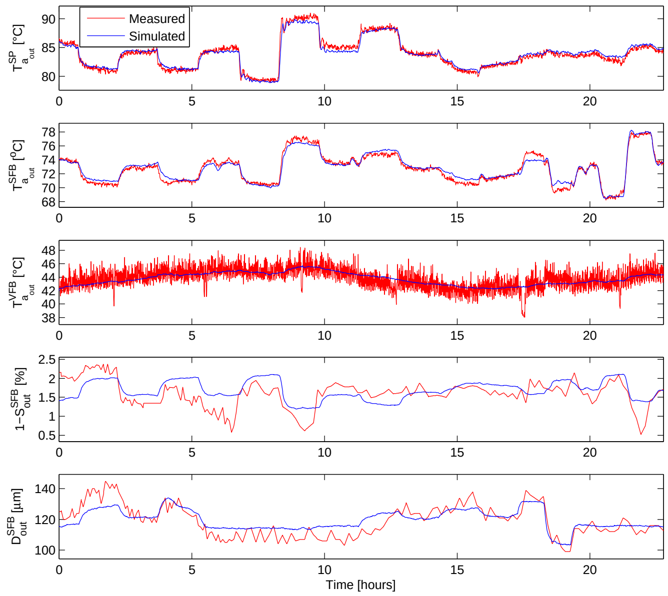

Fig. 4. The estimation dataset. S_{out}^{SFB} and D_{out}^{SFB} are sampled by hand resulting in a low sample frequency.

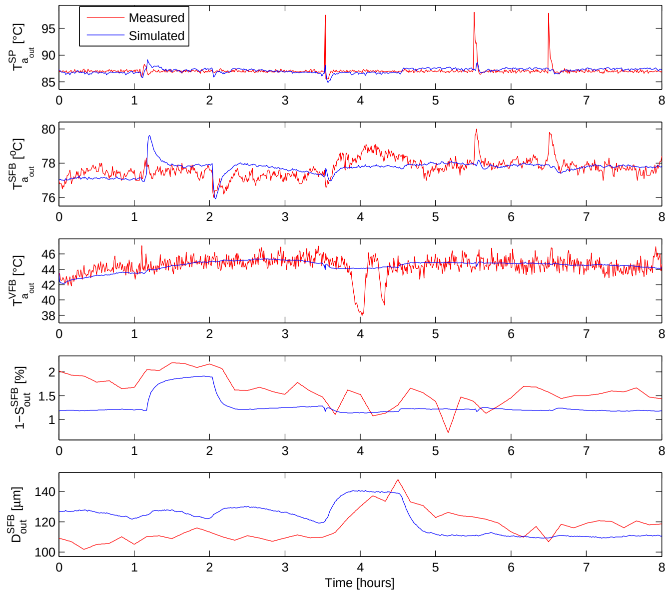

Fig. 5. The validation dataset. The three temperatures are offset corrected. The temperature peak ($t = 3.5$) is due to change of feed tank and the peak at $t = 5.5$ and 6.5 is due to change of nozzle.

5. CONCLUSIONS

In this paper, a mathematical model is proposed for a multi-stage spray dryer. We established a dynamic model consisting of three stages; the actual spray drying (SD), the static fluid bed (SFB) and the vibrating fluid bed (VFB). The stages were described by the same constitutive equation. The model predicts the temperatures within the dryer with high accuracy. The residual moisture and the particle size of the powder is predicted with some expected uncertainty, due to unstable discharge of powder from the SFB stage and varying indoor temperature. We also provided a novel prediction for stickiness of the powder, as a function of powder temperature and residual moisture. The model is general in the sense, that it can be adjusted to describe the drying of any liquid or slurry in a multi-stage spray dryer.

REFERENCES

Bizmark, N., Mostoufi, N., Sotudeh-Gharebagh, R., and Ehsani, H. (2010). Sequential modeling of fluidized bed paddy dryer. *Journal of Food Engineering*, 101, 303–308.

Chen, X.D. and Lin, S.X.Q. (2005). Air drying of milk droplet under constant and time-dependent conditions. *AIChE J.*, 51, 1790–1799.

Hennigs, C., Kockel, T.K., and Langrish, T.A.G. (2001). New measurements of the sticky behavior of skim milk powder. *Drying Technology*, 19, 471–484.

Hogan, S., Famelart, M., O'Callaghan, D., and Schuck, P. (2010). A novel technique for determining glass-rubber transition in dairy powders. *Journal of Food Engineering*, 99, 76–82.

Iguaz, A., Esnoz, A., Martínez, G., López, A., and Vírseda, P. (2003). Mathematical modelling and simulation for the drying process of vegetable wholesale by-products in a rotary dryer. *Journal of Food Engineering*, 59, 151–160.

IPTS and EuroCARE GmbH (2009). Economic impact of the abolition of the milk quota regime. URL `http://ec.europa.eu/agriculture/analysis/external/milkquota/ex_sum_en.pdf`.

Kristensen, N.R., Madsen, H., and Jørgensen, S.B. (2004). A method for systematic improvement of stochastic grey-box models. *Computers and Chemical Engineering*, 28, 1431–1449.

Langrish, T.A.G. and Kockel, T.K. (2001). The assessment of a characteristic drying curve for milk powder for use in computational fluid dynamics modelling. *Chemical Engineering Journal*, 84, 69–74.

Langrish, T.A.G. (2009). Multi-scale mathematical modelling of spray dryers. *Journal of Food Engineering*, 93, 218–228.

Ljung, L. (1999). *System Identification: Theory for the User (2nd Edition)*. Prentice Hall, Linkoping, Sweden.

O'Callaghan, D. and Cunningham, P. (2005). Modern process control techniques in the production of dried milk products - a review. *Lait*, 85, 335–342.

Shabde, V.S. and Hoo, K.A. (2008). Optimum controller design for a spray drying process. *Control Engineering Practice*, 16, 541–552.

Woo, M.W., Daud, W.R.W., Mujumdar, A.S., Wu, Z., Meor Talib, M.Z., and Tasirin, S.M. (2008). CFD evaluation of droplet drying models in a spray dryer fitted with a rotary atomizer. *Drying Technology*, 26, 1180–1198.

Appendix A. PRODUCT RELATED CONSTANTS

The latent heat of evaporation for water is $\lambda = 2260$ KJ. The heat capacity of dry air, vapour, solid maltodextrin DE-18 and water is

$$C_{da} = 1008.6 \qquad C_v = 1883.6$$

$$C_s = 1548.8 + 1.9625T - 5.9399 \cdot 10^{-3}T^2$$

$$C_w = 4176.2 - 0.0909T - 1.3129 \cdot 10^{-3}T^2$$